

Bilateral Output Feedback Control of Fractional PDEs with Space-Dependent Coefficients

Juan Chen* Aleksei Tepljakov** Eduard Petlenkov***
Bo Zhuang****

* Department of Computer Systems, Tallinn University of Technology,
Tallinn 19086, Estonia (e-mail: karenchenjuan.student@sina.com)

** Department of Computer Systems, Tallinn University of Technology,
Tallinn 19086, Estonia (e-mail: aleksei.tepljakov@taltech.ee)

*** Department of Computer Systems, Tallinn University of
Technology, Tallinn 19086, Estonia (e-mail:
eduard.petlenkov@taltech.ee)

**** School of Information Engineering, Binzhou University, Binzhou,
Shandong 256600, PR China (e-mail: sdzhuangbo@hotmail.com)

Abstract: This paper develops an extension of the bilateral control method for fractional partial differential equations (PDEs) with space-dependent coefficients by output feedback. Using a backstepping transformation, a full state feedback control law is designed. Then the fractional PDE system is folded into two subsystems and Mittag-Leffler convergent state observers of these subsystems are derived. Although the observers are coupled with boundary conditions (BCs), error subsystems are decoupled by assuming some available measurements. Hence, the observer gains are easily obtained. After this, we compose the designed state feedback controller and observers to enable Mittag-Leffler stabilization by output feedback. Finally, a fractional numerical example is provided to support the effectiveness of the proposed synthesis for the case when neither the control kernel nor the estimation kernel has an explicit solution.

Keywords: Fractional PDEs, bilateral output feedback control, space-dependent coefficients, Mittag-Leffler stability, backstepping.

1. INTRODUCTION

Recently, the boundary control of fractional partial differential equations (PDEs) has been got much attention after a breakthrough of the Mittag-Leffler stability (fractional Lyapunov stability) for fractional systems firstly proposed by Li et al. (2010). For the boundary stabilization problem of integer order PDEs, the backstepping method in Krstic and Smyshlyaev (2008) is a very useful tool. This has been shown to be suitable to the boundary control problem of fractional PDEs in Ge and Chen (2018), Chen et al. (2018a), Zhou and Guo (2018). It is worth to point out that, however, these works focus on the unilateral boundary control, i.e. a single controller at the boundary. The work in Vazquez and Krstic (2015) firstly induced the bilateral boundary control. There, the problem of stabilization of integer order PDEs in balls of arbitrary dimension is investigated. For a ball in 1-dimension, it is an interval and the boundaries are two ends. Subsequently, the research work on the bilateral boundary control of 1-dimensional PDEs was reported in Vazquez and Krstic

(2016). The results open a door for some other analogous works in integer order PDEs, from bilateral state feedback control in Chen et al. (2019); Auriol and Di Meglio (2017); Strecker and Aamo (2017), to (nonlinear) bilateral output feedback control in Bekiaris-Liberis and Vazquez (2019); Chen et al. (2019). Motivated by the above analysis, we concern the bilateral control method for fractional PDEs with space-dependent coefficients.

The main contribution of this paper is to achieve an initial result in bilateral output feedback control design for a fractional PDE with spatially-varying coefficients. We first develop the full-state feedback control design. By folding the original system into two subsystems, we design the observer of each subsystem separately. And the observers of the ‘folded’ systems are coupled, however, error subsystems are decoupled by assuming some available measurements. This makes simple to obtain the observer gains, which together with the proposed state feedback controller and observers results in a stabilizing output feedback control law.

The paper is organized as follows. In section 2, we introduce the considered problem. In section 3, we summarize the controller design for the fractional PDE system with spatially-varying coefficients by state feedback. Subsequently, we fold the original system into two sub-

* This publication is partially based upon works from COST Action CA15225, a network supported by COST (European Cooperation in Science and Technology), the Estonian Research Council grant PRG658, and National Natural Science Foundation of China (Grant Nos. 61807016).

systems and develop the corresponding observer design in Section 4. This results in an output feedback controller to enable the Mittag-Leffler stability of the closed-loop system. In section 5 and section 6, numerical simulations and some conclusions are presented respectively.

2. PROBLEM STATEMENT

In this paper, we consider the following fractional PDE system

$${}_0^C D_t^\alpha u(x, t) = a(x)u_{xx}(x, t) + \lambda(x)u(x, t), \quad (1)$$

$$u_x(-1, t) - bu(-1, t) = u_{1c}(t), \quad (2)$$

$$u_x(1, t) + qu(1, t) = u_{2c}(t) \quad (3)$$

for $(x, t) \in (-1, 1) \times \mathbb{R}^+$ with the initial condition (IC)

$$u(x, 0) = u_0(x), \quad x \in [0, 1],$$

where $a(x) > 0$, $x \in [-1, 1]$, $b, q \geq 0$, $u_{1c}(t)$, $u_{2c}(t)$ are the two-sided boundary control inputs and ${}_0^C D_t^\alpha(\cdot)$ is the Caputo time fractional derivative in Podlubny (1999)

$${}_0^C D_t^\alpha u(x, t) = \frac{1}{\Gamma(1-\alpha)} \int_0^t \frac{1}{(t-\tau)^\alpha} \frac{\partial u(x, \tau)}{\partial \tau} d\tau, 0 < \alpha < 1.$$

For the boundary conditions (BCs) (2)-(3), if $b = q = 0$, then BCs reduce to Neumann-type two-sided case. If $b, q \neq 0$, the BCs reduce to Robin-type two-sided case. Otherwise, the BCs become Mixed-type two-sided case. Without loss of generality, we only discuss the Robin-type bilateral case in this paper, and other cases are analogous. The following assumption is used in this paper:

Assumption 1. The system coefficients are sufficiently regular, in particular $a(x) = a(-x)$, $a(x) \in C^2[0, 1]$, $\lambda(x) \in C^1[0, 1]$.

Based on Assumption 1, we immediately get $a'(0) = 0$, which will be used later. Now recalling the results in Matignon (1996), we know that the original system (1)-(3) is potentially unstable. In this case, the control problem here is to design an appropriate boundary output feedback controller to make this system Mittag-Leffler stable. We refer Li et al. (2010) for more details on the Mittag-Leffler stability definition.

3. OVERVIEW OF STATE FEEDBACK CONTROL

3.1 Design of state feedback control

With the following transformation

$$w(x, t) = u(x, t) + \int_{-x}^x k(x, y)u(y, t)dy, \quad (4)$$

we map the original system (1)-(3) into the following target one

$${}_0^C D_t^\alpha w(x, t) = a(x)w_{xx}(x, t) - cw(x, t), \quad (5)$$

$$w_x(-1, t) - bw(-1, t) = 0, \quad (6)$$

$$w_x(1, t) + qw(1, t) = 0 \quad (7)$$

for $(x, t) \in (-1, 1) \times \mathbb{R}^+$ with the IC

$$w(x, 0) = w_0(x), \quad x \in [0, 1],$$

where $c > 0$. This target system is clearly Mittag-Leffler stable (see Theorem 1 for more details). Working out the kernel equations as in the one-sided boundary control case (see e.g. Chen et al. (2018a)), we get

$$a(x)k_{xx}(x, y) - (a(y)k(x, y))_{yy} = (\lambda(y) + c)k(x, y) \quad (8)$$

for $(x, y) \in [-1, 1] \times [-|x|, |x|]$ with BCs

$$2a(x)\frac{d}{dx}k(x, x) = -a'(x)k(x, x) + \lambda(x) + c, \quad (9)$$

$$k(x, -x) = 0 \quad (10)$$

by using the notation $\frac{d}{dx}k(x, -x) = k_x(x, -x) - k_y(x, -x)$ and Assumption 1. Note that here the computation of the kernel and the main proof of the stability for the case of bilateral boundary control can be viewed as an extension of the unilateral issue (e.g. Chen et al. (2018a)).

The well posedness of (8)-(10) will be discussed in Section 3.2. In this case, once the control kernel $k(x, y)$ exists, the control law can be given as follows

$$u_{1c}(t) = -k(-1, -1)u(-1, t) + \int_{-1}^1 k_x(-1, y)u(y, t)dy - \int_{-1}^1 bk(-1, y)u(y, t)dy, \quad (11)$$

$$u_{2c}(t) = -k(1, 1)u(1, t) - \int_{-1}^1 k_x(1, y)u(y, t)dy - \int_{-1}^1 qk(1, y)u(y, t)dy, \quad (12)$$

where we used $k(1, -1) = k(-1, 1) = 0$, calculated the space derivative of (4) (at $x = -1, 1$) and inserted this, (4) (at $x = -1, 1$) into (6)-(7) together with (2)-(3). To analyze the stability of the fractional PDE system (1)-(3), it is required that the transformation (4) is invertible. Let us introduce the following inverse transformation of kernel $l(x, y)$

$$u(x, t) = w(x, t) - \int_{-x}^x l(x, y)w(y, t)dy.$$

Proceeding as in the same lines used for k -kernel, it follows that l is governed by

$$a(x)l_{xx}(x, y) - (a(y)l(x, y))_{yy} = -(\lambda(x) + c)l(x, y)$$

for $(x, y) \in [-1, 1] \times [-|x|, |x|]$ with the BCs

$$2a(x)\frac{d}{dx}l(x, x) = -a'(x)l(x, x) + \lambda(x) + c,$$

$$l(x, -x) = 0.$$

This PDE is well-posed as long as the well posedness of kernel PDE (8)-(10) has been proved since they have a very similar structure.

The following theorem assesses the Mittag-Leffler stability of the closed-loop system (1)-(3), (11)-(12) under some conditions.

Theorem 1. For any initial values $u(x, 0) \in L^2(0, 1)$, the fractional PDE system (1)-(3) with the bilateral boundary control law (11)-(12) is L^2 Mittag-Leffler stable under the condition

$$\begin{cases} qa(1) + \frac{1}{2}a'(1) > 0, \\ ba(1) - \frac{1}{2}a'(-1) - \frac{1}{2}a_{\min} > 0, \\ c + \frac{1}{4}a_{\min} - \frac{1}{2}a''_{\max} > 0, \end{cases} \quad (13)$$

where $a''_{\max} = \max_{-1 \leq x \leq 1} \{a''(x)\}$, $a_{\min} = \min_{-1 \leq x \leq 1} \{a(x)\}$, $a'(x) = \frac{da(x)}{dx}$, and $a''(x) = \frac{d^2a(x)}{dx^2}$.

Proof. We start by considering a following Lyapunov functional

$$V_1(t) = \frac{1}{2} \int_{-1}^1 w^2(x, t) dx.$$

Then taking its Caputo time fractional derivative and applying Lemma 1 in Aguila-Camacho et al. (2014), it follows that

$$\begin{aligned} & {}_0^C D_t^\alpha V_1(t) \\ & \leq -\left(qa(1) + \frac{1}{2} a'(1) \right) w^2(1, t) - \left(ba(1) - \frac{1}{2} a'(-1) - \frac{1}{2} \right. \\ & \quad \left. \times a_{\min} \right) w^2(-1, t) - \left(c + \frac{a_{\min}}{4} - \frac{a''_{\max}}{2} \right) \int_{-1}^1 w^2(x, t) dx \end{aligned}$$

by employing the formula $\int_{-1}^1 a'(x) w(x, t) dw(x, t) = \frac{1}{2} \left(a'(1) w^2(1, t) - a'(-1) w^2(-1, t) - \int_{-1}^1 a''(x) w^2(x, t) dx \right)$, the integration by parts, Poincaré inequality (see Lemma 2.1 in Krstic and Smyshlyaev (2008)), and BCs (6)-(7). Recalling the condition (13), we immediately get

$${}_0^C D_t^\alpha V_1(t) \leq -2m_1 V_1(t), \quad (14)$$

where $m_1 = c + \frac{1}{4} a_{\min} - \frac{1}{2} a''_{\max}$.

With (14) and the fractional extension of Lyapounov method in Li et al. (2010), one immediately gets

$$\begin{aligned} V_1(t) & := V_1(t, w(\cdot, t)) \\ & = V_1(0, w(\cdot, 0)) E_\alpha(-2m_1 t^\alpha) \\ & \quad + \int_0^t \frac{E_{\alpha, \alpha}(-2m_1(t-s)^\alpha)}{(t-s)^{1-\alpha}} N(s) ds \end{aligned}$$

where $N(t) = {}_0^C D_t^\alpha V_1 + 2m_1 V_1 \leq 0$, $E_{\alpha, \beta}(z) := \sum_{k=0}^{\infty} \frac{z^k}{\Gamma(\alpha k + \beta)}$, $\alpha, \beta > 0$, $E_\alpha(z) := E_{\alpha, 1}(z)$. Using $E_{\alpha, \alpha}(-2m_1 t^\alpha) \geq 0$, when $\alpha > 0$, $m_1 > 0$, it follows that

$$V_1(t) \leq V_1(0, w(\cdot, 0)) E_\alpha(-2m_1 t^\alpha),$$

which implies

$$\|w(\cdot, t)\| \leq [2V_1(0, w(\cdot, 0)) E_\alpha(-2m_1 t^\alpha)]^{1/2}.$$

By the definition of Mittag-Leffler stability in Li et al. (2010), we then obtain the system (5)-(7) is Mittag-Leffler stable. This composes with the invertibility of (4) to imply the L^2 Mittag-Leffler stability of (1)-(3), (11)-(12).

3.2 Analysis of control kernel

We introduce the following changes of variables

$$\check{k}(\check{x}, \check{y}) = a^{-1/4}(x) a^{3/4}(y) k(x, y),$$

$$\check{x} = \psi(x), \check{y} = \psi(y), \psi(\mu) = \sqrt{a(0)} \int_{-\mu}^{\mu} \frac{d\tau}{\sqrt{a(\tau)}},$$

$$G(\xi, \eta) = \check{k}\left(\frac{\xi + \eta}{2}, \frac{\xi - \eta}{2}\right),$$

$$\xi = \check{x} + \check{y}, \eta = \check{x} - \check{y},$$

then the kernel PDE (8)-(10) becomes

$$G_{\xi\eta}(\xi, \eta) = \frac{\check{\phi}\left(\frac{\xi+\eta}{2}, \frac{\xi-\eta}{2}\right)}{16a(0)} G(\xi, \eta), \quad (15)$$

$$G_\xi(\xi, 0) = \frac{1}{8\sqrt{a(0)}} \left(\lambda\left(\psi^{-1}\left(\frac{\xi}{2}\right)\right) + c \right), \quad (16)$$

$$G(0, \eta) = 0, \quad (17)$$

where $\check{\phi}\left(\frac{\xi+\eta}{2}, \frac{\xi-\eta}{2}\right) = \check{\phi}(\check{x}, \check{y}) = \frac{3}{16} \left(\frac{a_i'^2(x)}{a_i(x)} - \frac{a_i'^2(y)}{a_i(y)} \right) + \frac{1}{4} (a_i''(y) - a_i''(x)) + \lambda(x) + c$. This PDE (15)-(17) can be

transformed into an integral equation and then applying the method of successive approximations (as in Chen et al. (2017)). We thus can obtain the well posedness of (8)-(10).

Remark 1. Note that $\psi(\mu)$ (lower bound) is slightly different from the one in Smyshlyaev and Krstic (2005) since the problem here is a case of the bilateral boundary control rather than a unilateral case.

4. OUTPUT FEEDBACK CONTROL

4.1 Folding of system and observer design of subsystems

We now ‘fold’ the system (1)-(3) into two subsystem u_1, u_2 , i.e.

$${}_0^C D_t^\alpha u_1(x, t) = a(x) u_{1xx}(x, t) + \lambda_1(x) u_1(x, t), \quad (18)$$

$$u_1(0, t) = u_2(0, t), \quad (19)$$

$$u_{1x}(1, t) + q u_1(1, t) = u_{2c}(t), \quad (20)$$

$${}_0^C D_t^\alpha u_2(x, t) = a(x) u_{2xx}(x, t) + \lambda_2(x) u_2(x, t), \quad (21)$$

$$u_{2x}(0, t) = -u_{1x}(0, t), \quad (22)$$

$$u_{2x}(1, t) + b u_2(1, t) = -u_{1c}(t) \quad (23)$$

for $(x, t) \in (0, 1) \times \mathbb{R}^+$ with ICs

$$u_1(x, 0) = u_{10}(x), u_2(x, 0) = u_{20}(x), \quad x \in [0, 1],$$

where $u_1(x, t) := u(x, t)$, $u_2(x, t) := u(-x, t)$, $\lambda_1(x) := \lambda(x)$, $\lambda_2(x) := \lambda(-x)$, $0 \leq x \leq 1$. Note that the ‘folded’ systems u_1, u_2 are coupled through the exotic BCs coupling the systems.

Here we assume availability of $u_{1x}(0, t)$, $u_2(0, t)$ for measurement. Then the corresponding observers are copied by u_1, u_2 with the correction terms, i.e.

$${}_0^C D_t^\alpha \hat{u}_1(x, t) = a(x) \hat{u}_{1xx}(x, t) + \lambda_1(x) \hat{u}_1(x, t) + r_1(x) \quad (24)$$

$$\hat{u}_1(0, t) = u_2(0, t) + r_{10}(u_{1x}(0, t) - \hat{u}_{1x}(0, t)), \quad (25)$$

$$\hat{u}_{1x}(1, t) + q \hat{u}_1(1, t) = u_{2c}(t), \quad (26)$$

$$\begin{aligned} & {}_0^C D_t^\alpha \hat{u}_2(x, t) = a(x) \hat{u}_{2xx}(x, t) + \lambda_2(x) \hat{u}_2(x, t) + r_2(x) \\ & \quad \times (u_2(0, t) - \hat{u}_2(0, t)), \end{aligned} \quad (27)$$

$$\hat{u}_{2x}(0, t) = -u_{1x}(0, t) + r_{20}(u_2(0, t) - \hat{u}_2(0, t)), \quad (28)$$

$$\hat{u}_{2x}(1, t) + b \hat{u}_2(1, t) = -u_{1c}(t), \quad (29)$$

for $(x, t) \in (0, 1) \times \mathbb{R}^+$ with ICs

$$\hat{u}_1(x, 0) = \hat{u}_{10}(x), \hat{u}_2(x, 0) = \hat{u}_{20}(x), x \in [0, 1],$$

where the observer gains $r_i(x), r_{i0}$ will be designed later, $i = 1, 2$.

Remark 2. In this paper, the correction term and observer gains induce the different structures of \hat{u}_1, \hat{u}_2 , and \tilde{u}_1, \tilde{u}_2 , which are completely different from the one in Chen et al. (2019). There, \hat{u}_1, \hat{u}_2 , and \tilde{u}_1, \tilde{u}_2 have the same structure that is a special one rather than a more general one here.

Let $\tilde{u}_i(x, t) = u_i(x, t) - \hat{u}_i(x, t), i = 1, 2$, then we have the error subsystems

$$\begin{aligned} & {}_0^C D_t^\alpha \tilde{u}_1(x, t) = a(x) \tilde{u}_{1xx}(x, t) + \lambda_1(x) \tilde{u}_1(x, t) - r_1(x) \\ & \quad \times \tilde{u}_{1x}(0, t), \end{aligned} \quad (30)$$

$$\tilde{u}_1(0, t) = -r_{10} \tilde{u}_{1x}(0, t), \quad (31)$$

$$\tilde{u}_{1x}(1, t) + q \tilde{u}_1(1, t) = 0, \quad (32)$$

$$\begin{aligned} & {}_0^C D_t^\alpha \tilde{u}_2(x, t) = a(x) \tilde{u}_{2xx}(x, t) + \lambda_2(x) \tilde{u}_2(x, t) - r_2(x) \\ & \quad \times \tilde{u}_2(0, t), \end{aligned} \quad (33)$$

$$\tilde{u}_{2x}(0, t) = -r_{20} \tilde{u}_2(0, t), \quad (34)$$

$$\tilde{u}_{2x}(1, t) + b \tilde{u}_2(1, t) = 0 \quad (35)$$

for $(x, t) \in (0, 1) \times \mathbb{R}^+$ with ICs

$$\tilde{u}_1(x, 0) = \tilde{u}_{10}(x), \tilde{u}_2(x, 0) = \tilde{u}_{20}(x), \quad x \in [0, 1].$$

Remark 3. It is worth to point out that since the measurement of $u_{1x}(0, t)$, $u_2(0, t)$ is available, error subsystems (30)-(32), (33)-(35) are decoupled. This makes observer gains design of each one simple, which is inspired by Moura et al. (2013).

We employ the following transformation

$$\tilde{u}_1(x, t) = \tilde{w}_1(x, t) + \int_0^x p_1(x, y) \tilde{w}_1(y, t) dy \quad (36)$$

$$\tilde{u}_2(x, t) = \tilde{w}_2(x, t) + \int_0^x p_2(x, y) \tilde{w}_2(y, t) dy \quad (37)$$

to map the error subsystems (30)-(32), (33)-(35) into the target ones

$${}_0^C D_t^\alpha \tilde{w}_1(x, t) = a(x) \tilde{w}_{1xx}(x, t) - \tilde{c}_1 \tilde{w}_1(x, t), \quad (38)$$

$$\tilde{w}_1(0, t) = 0, \quad (39)$$

$$\tilde{w}_{1x}(1, t) + q \tilde{w}_1(1, t) = 0, \quad (40)$$

$${}_0^C D_t^\alpha \tilde{w}_2(x, t) = a(x) \tilde{w}_{2xx}(x, t) - \tilde{c}_2 \tilde{w}_2(x, t), \quad (41)$$

$$\tilde{w}_{2x}(0, t) = 0, \quad (42)$$

$$\tilde{w}_{2x}(1, t) + b \tilde{w}_2(1, t) = 0 \quad (43)$$

for $(x, t) \in (0, 1) \times \mathbb{R}^+$ with ICs

$$\tilde{w}_1(x, 0) = \tilde{w}_{10}(x), \tilde{w}_2(x, 0) = \tilde{w}_{20}(x), \quad x \in [0, 1],$$

where $\tilde{c}_1, \tilde{c}_2 > 0$.

After same lengthly computations as in Section 3.1, we get that kernels p_1, p_2 are governed by

$$a(x) p_{1xx}(x, y) - (a(y) p_1(x, y))_{yy} = -(\lambda_1(x) + \tilde{c}_1) p_1(x, y), \quad (44)$$

$$2a(x) \frac{d}{dx} p_1(x, x) = -a'(x) p_1(x, x) - \lambda_1(x) - \tilde{c}_1, \quad (45)$$

$$p_{1x}(1, y) = -q p_1(1, y), \quad (46)$$

$$p_1(1, 1) = 0, \quad (47)$$

$$a(x) p_{2xx}(x, y) - (a(y) p_2(x, y))_{yy} = -(\lambda_2(x) + \tilde{c}_2) p_2(x, y) \quad (48)$$

$$2a(x) \frac{d}{dx} p_2(x, x) = -a'(x) p_2(x, x) - \lambda_2(x) - \tilde{c}_2, \quad (49)$$

$$p_{2x}(1, y) = -b p_2(1, y), \quad (50)$$

$$p_2(1, 1) = 0 \quad (51)$$

for $0 \leq y \leq x \leq 1$ in (44) and (48), and observer gains should be chosen as

$$r_1(x) = a(0) p_1(x, 0), r_{10} = 0, \quad (52)$$

$$r_2(x) = -a(0) p_{2y}(x, 0) - a'(0) p_2(x, 0),$$

$$r_{20} = -p_2(0, 0). \quad (53)$$

Due to $a'(0) = 0$, $r_2(x)$ actually reduces to

$$r_2(x) = -a(0) p_{2y}(x, 0). \quad (54)$$

We next provide the below lemmas to conclude the well posedness of p_1 -kernel equations (44)-(47) and p_2 -kernel equations (48)-(51).

Lemma 2. The kernel PDE (44)-(47) has a unique solution which is twice continuously differentiable in $0 \leq y \leq x \leq 1$.

Proof. We start with a change of variables

$$\bar{p}_1(\bar{x}, \bar{y}) = p_1(x, y), \bar{a}(\bar{y}) = a(x),$$

$$\bar{\lambda}_1(\bar{y}) = \lambda_1(x), \bar{x} = 1 - y, \bar{y} = 1 - x.$$

Then the equation (44)-(47) converts into

$$\begin{aligned} \bar{a}(\bar{y}) \bar{p}_{1\bar{y}\bar{y}}(\bar{x}, \bar{y}) - (\bar{a}(\bar{x}) \bar{p}_1(\bar{x}, \bar{y}))_{\bar{x}\bar{x}} &= -(\bar{\lambda}_1(\bar{y}) + \tilde{c}_1) \\ &\times \bar{p}_1(\bar{x}, \bar{y}) \end{aligned} \quad (55)$$

for $0 \leq \bar{y} \leq \bar{x} \leq 1$ with the BCs

$$2\bar{a}(\bar{y}) \frac{d}{d\bar{y}} \bar{p}_1(\bar{y}, \bar{y}) = -\bar{p}_1(\bar{y}, \bar{y}) \bar{a}'(\bar{y}) + \bar{\lambda}_1(\bar{y}) + \tilde{c}_1, \quad (56)$$

$$\bar{p}_{1\bar{y}}(\bar{x}, 0) = q \bar{p}_1(\bar{x}, 0), \quad (57)$$

$$\bar{p}_1(0, 0) = 0. \quad (58)$$

Interestingly, (55)-(58) is in class PDE (21) in Chen et al. (2018a). Hence, using Lemma 1 in Chen et al. (2018a), we can immediately obtain the result here. This concludes our proof.

Lemma 3. The kernel PDE (48)-(51) has a unique C^2 solution in $0 \leq y \leq x \leq 1$.

Proof. Very similar to the proof of Lemma 2.

4.2 Mittag-Leffler convergence analysis of observers

The problem is to design a Mittag-Leffler convergent observer for the plant, in the sense that, to prove the Mittag-Leffler stability of observer error systems. For the stability of (30)-(35), it is required that the transformations (36),(37) are invertible. This, in fact, can be derived from Lemma 3 in Chen et al. (2018b). Now the following main results hold for boundary observers.

Theorem 4. Given the u_1 -subsystem (18)-(20) with initial value $u_1(x, 0) \in L^2(0, 1)$, the observer (24)-(26) with (52) and the initial value $\hat{u}_1(x, 0) \in L^2(0, 1)$ is Mittag-Leffler convergent under the condition

$$\begin{cases} qa(1) + \frac{1}{2}a'(1) > 0, \\ \tilde{c}_1 + \frac{1}{4}\tilde{a}_{\min} - \frac{1}{2}\tilde{a}_{\max}'' > 0, \end{cases} \quad (59)$$

where $\tilde{a}_{\min} = \min_{0 \leq x \leq 1} \{a(x)\}$, $\tilde{a}_{\max}'' = \max_{0 \leq x \leq 1} \{a''(x)\}$.

Proof. We consider a Lyapunov functional as follows:

$$V_2(t) = \frac{1}{2} \int_0^1 \tilde{w}_1^2(x, t) dx. \quad (60)$$

Taking the Caputo time fractional derivative of (60) and using Lemma 1 in Aguila-Camacho et al. (2014) yields,

$$\begin{aligned} &{}_0^C D_t^\alpha V_2(t) \\ &\leq -\left(qa(1) + \frac{1}{2}a'(1)\right) \tilde{w}_1^2(1, t) - \left(\tilde{c}_1 + \frac{1}{4}\tilde{a}_{\min} - \frac{1}{2}\tilde{a}_{\max}''\right) \\ &\quad \times \int_0^1 \tilde{w}_1^2(x, t) dx, \end{aligned}$$

where we used the formula $\int_0^1 a'(x) \tilde{w}_1(x, t) d\tilde{w}_1(x, t) = \frac{1}{2}a'(1) \tilde{w}_1^2(1, t) - \frac{1}{2} \int_0^1 a''(x) \tilde{w}_1^2(x, t) dx$, Poincaré inequality, the integration by parts, and BCs (39)-(40). With the condition (59), we further have

$${}_0^C D_t^\alpha V_2(t) \leq -2m_2 V_2(t),$$

where $m_2 = \tilde{c}_1 + \frac{1}{4}\tilde{a}_{\min} - \frac{1}{2}\tilde{a}_{\max}''$. Proceeding as the same procedure in the proof of Theorem 1, we can obtain the Mittag-Leffler stability of (38)-(40). This, together with the invertibility of (36), implies that (30)-(32) is L^2 Mittag-Leffler stable which induces our result here.

Theorem 5. Consider the u_2 -subsystem (21)-(23) with initial value $u_2(x, 0) \in L^2(0, 1)$, the observer (27)-(29) with (54), (53) and the initial value $\hat{u}_2(x, 0) \in L^2(0, 1)$ is Mittag-Leffler convergent under the condition

$$\begin{cases} a'(0) = 0, \\ ba(1) + \frac{1}{2}a'(1) - \frac{1}{2}\tilde{a}_{\min} > 0, \\ \tilde{c}_2 + \frac{1}{4}\tilde{a}_{\min} - \frac{1}{2}\tilde{a}_{\max}'' > 0. \end{cases} \quad (61)$$

Proof. The proof is omitted but follows directly from the consideration of a Lyapunov functional $V_3(t) = \frac{1}{2} \int_0^1 \tilde{w}_2^2(x, t) dx$ along the solution of (41)-(43) together with the invertibility of (37).

4.3 Output feedback Mittag-Leffler stabilization

We combine the observers with backstepping controllers to solve the output feedback control problem. The main result will be presented as follows.

Theorem 6. Let $k(-1, y)$, $k_x(-1, y)$, $k(1, y)$, $k_x(1, y)$ be solutions of (8)-(10), and let $r_i(x)$, r_{i0} , $i = 1, 2$ be derived from (52)-(54), (44)-(51). Then for any initial values $u(x, 0)$, $\hat{u}(x, 0) \in L^2(0, 1)$, the system (1)-(3) with the controller

$$\begin{aligned} u_{1c}(t) = & -k(-1, -1)\hat{u}(-1, t) + \int_{-1}^1 k_x(-1, y)\hat{u}(y, t)dy \\ & - \int_{-1}^1 bk(-1, y)\hat{u}(y, t)dy, \end{aligned} \quad (62)$$

$$\begin{aligned} u_{2c}(t) = & -k(1, 1)\hat{u}(1, t) - \int_{-1}^1 k_x(1, y)\hat{u}(y, t)dy \\ & - \int_{-1}^1 qk(1, y)\hat{u}(y, t)dy, \end{aligned} \quad (63)$$

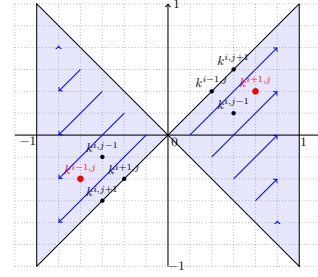
and the observers (24)-(29) is L^2 Mittag-Leffler stable under the conditions (13), (59), (61).

Proof. Theorem 4, Theorem 5 yields the convergence of observer error states \tilde{u}_1 , \tilde{u}_2 to zero. Hence, we have $u_{1x}(0, t)$, $u_2(0, t)$ converge to $\hat{u}_{1x}(0, t)$, $\hat{u}_2(0, t)$ respectively. Then we can apply Theorem 1 to observers (24)-(29). We thus obtain $(\tilde{u}_1, \tilde{u}_2, \hat{u}_1, \hat{u}_2)$ are Mittag-Leffler stable, which implies the closed-loop stability of (u_1, u_2) .

5. SIMULATION STUDY

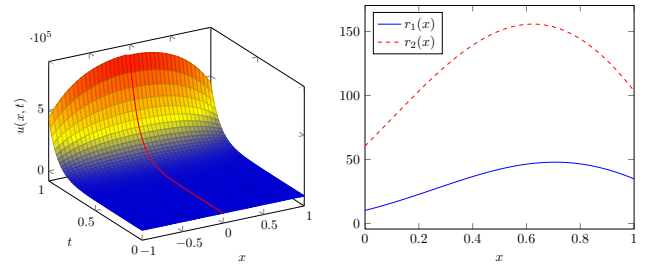
In this section, we provide a fractional numerical example to support the theoretical results of the bilateral boundary control by output feedback. Here the modified numerical algorithm of Caputo time fractional-order derivative derived from Li et al. (2016) is utilized to discretize the spatial and time domains for the fractional PDE system (1)-(3). It is worth to point out that the explicit solution of the kernel PDE (8)-(10) is not available, we thus solve it numerically. In this case, the simulation scheme is developed as follows:

$$\begin{aligned} k^{i+1, j} = & \frac{1}{a_j} [(2(a_i - a_j) + h^2(\lambda_i + c))\hat{k}^{ij} + a_{j+1}k^{i, j+1} \\ & + a_{j-1}k^{i, j-1}] - k^{i-1, j}, \\ i = & M + 2, \dots, 2M, j = 2, \dots, 2M, \end{aligned}$$



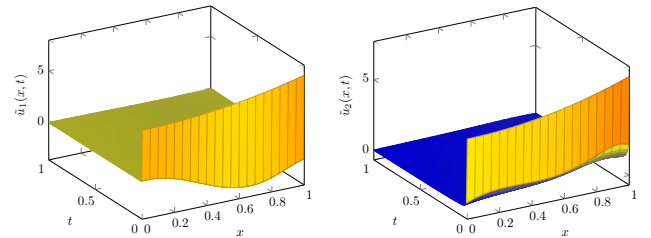
(a)

Fig. 1. Schematic computational implementation of kernel $k(x, y)$.



(a)

(b)



(c)

(d)

Fig. 2. Open-loop response of the fractional PDE system (1)-(3), observer gains $r_1(x)$, $r_2(x)$, and state profiles of error subsystems (30)-(32), (33)-(35).

$$\begin{aligned} k^{i+1, i+1} = & \frac{1}{1 + \frac{ha'_{i+1}}{4a_{i+1}}} \left(\left(1 - \frac{ha'_i}{4a_i} \right) + \frac{h}{4} \left(\frac{\lambda_{i+1} + c}{a_{i+1}} \right. \right. \\ & \left. \left. + \frac{\lambda_i + c}{a_i} \right) \right), i = M + 1, \dots, 2M \end{aligned}$$

for $x \geq 0$. It is clear that the numerical solution of kernel $k(x, y)$ in the case $x \leq 0$ is quite straightforward by a symmetry argument. Here, $k^{ij} = k(x_i, y_j)$, $a_i = a(x_i)$, $\lambda_i = \lambda(x_i)$, $\hat{k}^{ij} := (k^{i, j+1} + k^{i, j-1})/2$, $h = 1/M$, M is the number of steps. In order to illustrate the principle setup, we show the computational realization in Figure 1.

The kernels $p_1(x, y)$ and $p_2(x, y)$ are also solved numerically, whose computational realization is similar to the one of $k(x, y)$. Consider a fractional PDE system (1)-(3), (62), (63), (24)-(29) with system parameters $a(x) = (1 - \frac{1}{2}x^2)^2$, $\lambda(x) = x^2 + 6$, $c = 8$, $\lambda_1(x) = \lambda_2(x) = x^2 + 6$, $\tilde{c}_1 = 10$, $\tilde{c}_2 = 10$, $q = 2.5$, $b = 2.6$, and initial values $u(x, 0) = 4x^2 + 6$, $\hat{u}_1(x, 0) = \hat{u}_2(x, 0) = 2x^2 + 1$. Clearly, the conditions (13), (59), (61) hold true with these parameters. Figure 2 shows the open-loop unstable, observer gains $r_1(x)$, $r_2(x)$, and the state evolution of error subsystems (30)-(32), (33)-(35). In Figure 3, control kernels, the control effort, state profiles, and the state L^2 -norm of the closed-loop system

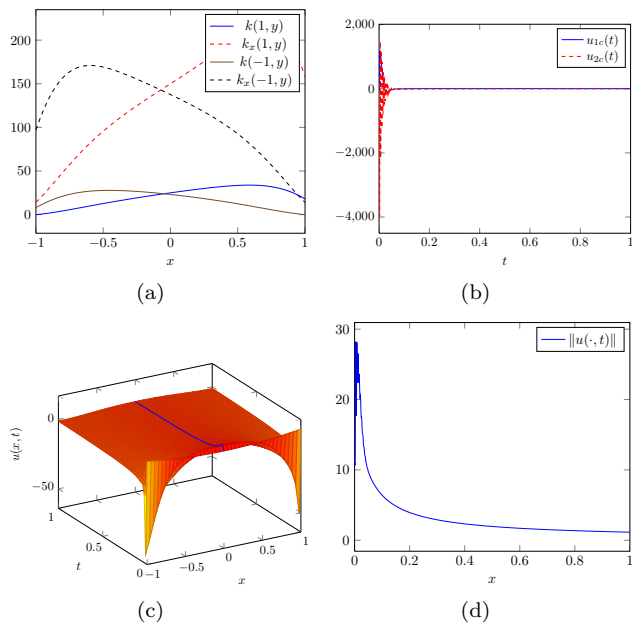


Fig. 3. Control kernel, control efforts, and closed-loop response of the fractional PDE system (1)-(3), (62)-(63), (24)-(29) by output feedback.

are pictured. As we expected, the bilateral boundary controller (62)-(63) makes the fractional closed-loop system Mittag-Leffler stable. Note that the ‘folding’ point is at the point of symmetry $x = 0$, which has been marked in red and blue in Figure 2 (a) and Figure 3 (c).

6. CONCLUSION

In this paper, we extended the backstepping method to the fractional PDE with the bilateral boundary control and spatially-varying coefficients. Generally speaking, we first derived the full-state feedback control law, then folded the original system into subsystems and designed the observers for them. We here assume the availability of $u_{1x}(0, t)$, $u_2(0, t)$ for measurement to make the BCs of error subsystems are decoupled. In this case, we can obtain the observer gains easily. Then the observer-based output feedback controllers are derived to enable Mittag-Leffler stabilization of the closed-loop system. The present paper is a continuation of the results in Chen et al. (2018a), and it could be interesting to see how to apply the bilateral control to fractional PDE-fractional ODE cascades or coupled fractional PDEs with space-dependent parameters.

REFERENCES

Aguila-Camacho, N., Duarte-Mermoud, M.A., and Gallegos, J.A. (2014). Lyapunov functions for fractional order systems. *Communications in Nonlinear Science and Numerical Simulation*, 19(9), 2951–2957.

Auriol, J. and Di Meglio, F. (2017). Two-sided boundary stabilization of heterodirectional linear coupled hyperbolic PDEs. *IEEE Transactions on Automatic Control*, 63(8), 2421–2436.

Bekiaris-Liberis, N. and Vazquez, R. (2019). Nonlinear bilateral output-feedback control for a class of viscous Hamilton-Jacobi PDEs. *Automatica*, 101, 223–231.

Chen, J., Cui, B., and Chen, Y. (2018a). Backstepping-based boundary control design for a fractional reaction diffusion system with a space-dependent diffusion coefficient. *ISA Transactions*, 80, 203–211.

Chen, J., Cui, B., and Chen, Y. (2018b). Observer-based output feedback control for a boundary controlled fractional reaction diffusion system with spatially-varying diffusivity. *IET Control Theory & Applications*, 12(11), 1561–1572.

Chen, J., Zhuang, B., Chen, Y., and Cui, B. (2017). Backstepping-based boundary feedback control for a fractional reaction diffusion system with mixed or Robin boundary conditions. *IET Control Theory & Applications*, 11(17), 2964–2976.

Chen, S., Vazquez, R., and Krstic, M. (2019). Folding backstepping approach to parabolic PDE bilateral boundary control. *IFAC-PapersOnLine*, 52(2), 76–81.

Ge, F. and Chen, Y. (2018). Event-driven boundary control for time fractional diffusion systems under time-varying input disturbance. In *American Control Conference (ACC)*, 140–145. IEEE.

Krstic, M. and Smyshlyaev, A. (2008). *Boundary Control of PDEs: A Course on Backstepping Designs*. Society for Industrial and Applied Mathematics.

Li, H., Cao, J., and Li, C. (2016). High-order approximation to Caputo derivatives and Caputo-type advection-diffusion equations (III). *Journal of Computational & Applied Mathematics*, 299(3), 159–175.

Li, Y., Chen, Y., and Podlubny, I. (2010). Stability of fractional-order nonlinear dynamic systems: Lyapunov direct method and generalized Mittag-Leffler stability. *Computers & Mathematics with Applications*, 59(5), 1810–1821.

Matignon, D. (1996). Stability results for fractional differential equations with applications to control processing. *Computational Engineering in Systems Applications*, 2, 963–968.

Moura, S., Bendtsen, J., and Ruiz, V. (2013). Observer design for boundary coupled PDEs: Application to thermostatically controlled loads in smart grids. In *2013 IEEE Conference on Decision and Control*, 6286–6291. IEEE.

Podlubny, I. (1999). *Fractional differential equations*. Academic press, San Diego, CA.

Smyshlyaev, A. and Krstic, M. (2005). On control design for PDEs with space-dependent diffusivity or time-dependent reactivity. *Automatica*, 41(9), 1601–1608.

Strecker, T. and Aamo, O.M. (2017). Two-sided boundary control and state estimation of 2×2 semilinear hyperbolic systems. In *2017 IEEE Conference on Decision and Control (CDC)*, 2511–2518. IEEE.

Vazquez, R. and Krstic, M. (2015). Boundary control of reaction-diffusion PDEs on balls in spaces of arbitrary dimensions. *arXiv preprint arXiv:1511.06641*.

Vazquez, R. and Krstic, M. (2016). Bilateral boundary control of one-dimensional first-and second-order PDEs using infinite-dimensional backstepping. In *2016 IEEE Conference on Decision and Control (CDC)*, 537–542. IEEE.

Zhou, H.C. and Guo, B.Z. (2018). Boundary feedback stabilization for an unstable time fractional reaction diffusion equation. *SIAM Journal on Control and Optimization*, 56(1), 75–101.